Interwell coherent tunneling in coupled quantum wells

C. Juang
Materials Research Laboratories, ITRI, Hsinchu, Taiwan 31015, Republic of China
(Received 17 December 1990; revised manuscript received 15 July 1991)

A theoretical investigation of interwell coherent tunneling in coupled quantum wells is presented. The time-dependent picture of coherent tunneling of an electron wave packet is obtained by the application of the time-development operator of the time-dependent Schrödinger equation. The interwell tunneling is shown for under bias, resonance, and over bias conditions. In addition, the tunneling probability and tunneling time based on this time-dependent analysis are calculated. This method improves upon the conventional model that is currently in use for the coherent tunneling in coupled quantum wells.

I. INTRODUCTION

The investigation of the quantum-mechanical properties in coupled quantum wells, which consist of two quantum wells located sufficiently close together, has been a subject of much interest.[1–8] Steady-state properties such as energy states and field-induced energy shifts in coupled quantum wells have been studied. For example, symmetric and antisymmetric energy levels in symmetric coupled wells have been reported.[1,2] An enhancement of the quantum-confined Stark effect due to the coupling of electronic levels in coupled quantum wells has been observed.[3,4]

More recently, one dynamic property of field-induced interwell electron tunneling in coupled quantum wells has attracted some attention.[5–8] For a particle initially confined in one of the wells, interwell tunneling occurs with an applied field. If the energy levels in both wells are far apart ($|\Delta E|>0$), the tunneling is of the nonresonant type. If the energy levels in both wells are very close to each other ($|\Delta E|\sim 0$), then resonant tunneling occurs. By changing the external electric field across coupled quantum wells, the resonant condition can be achieved. Figure 1 illustrates under bias, resonance, and over bias conditions in coupled quantum wells due to the external electric field. At resonance, a reduction of tunneling time has been observed by time-resolved photocurrent measurements[5] and by time-resolved photoluminescence measurements.[6,7] The coherent-tunneling time obtained by the conventional model, $h/2|\Delta E|$, has been compared to the experimental results.[6,7] There are

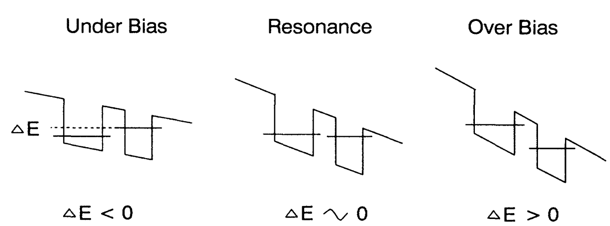

FIG. 1. Schematic potential profiles of coupled quantum wells under an external electric field at under bias, resonance, and over bias conditions.

two discrepancies: (1) the measured tunneling time is much longer than the coherent-tunneling time obtained by the conventional model, and (2) at resonance, the tunneling time should be longer (not a reduction of tunneling time as the measured results reported) than that at nonresonance since $|\Delta E|$ is smaller at resonance. Due to these discrepancies, some have attributed the resonant effect to phonon-assisted tunneling.[7,8]

However, the conventional model needs to be examined more carefully. This model is used to calculate the tunneling time in symmetric coupled quantum wells.[9] The energy difference between the ground states of each well in symmetric coupled quantum wells is obtained using first-order perturbation theory which requires a small $|\Delta E|$. At nonresonance, energy differences are large; therefore, the discrepancies in the model are obvious. In addition, electric-field effects are not taken into consideration in the model. This limits the use of the model in electric-field-control tunneling effects. Also, the tunneling time is obtained from the phase change in time, which is inappropriate to describe the spatial-tunneling effects in coupled quantum wells since the phase factor is canceled out when considering the probability distribution function $|\phi|^2$. More importantly, the tunneling time is expected to be strongly influenced by the barrier width. However, this is also overlooked by the conventional model. Thus a more detailed description of the interwell coherent tunneling is needed to give a better insight into the coherent-tunneling mechanism.

The purpose of this paper is to improve upon the conventional model by (1) showing both resonant and nonresonant effects, (2) including the external electric field, and (3) using the probability distribution function $|\phi|^2$ to describe the spatial tunneling effect. The approach of this work is to describe the field-induced interwell coherent tunneling in coupled quantum wells by the application of the time-development operator according to the time-dependent Schrödinger equation while the Stark shift in each well is determined using the time-independent Schrödinger equation solved by the inverse-power method.[10] Field-induced tunneling in single quantum wells (tunnel out of quantum wells) has been described by this time-dependent analysis. The same approach is equally valid in the treatment of the field-induced interwell coherent tunneling. The evolutions of the particles are shown at under bias, at resonance, and over bias conditions. The tunneling probability based on this time-dependent analysis is also calculated for various barrier widths. It is found that the particle not only tunnels to the second well but also tunnels back to the first well. At nonresonance, only a very small portion of the wave packet ever tunnels into the second well. In addition, the tunneling time based on the time-dependent analysis is compared to that obtained by the conventional model.

Section II summarized the numerical techniques for solving the time-dependent and the time-independent Schrödinger equations. The interwell coherent tunneling in coupled quantum wells is shown in Sec. III. The tunneling probabilities at under bias, resonance, and over bias conditions are obtained for various barrier widths. Section IV compares the conventional model to the time-dependent analysis. The shortcomings of the conventional model will also be discussed.

II. METHOD OF NUMERICAL ANALYSIS

To show the field-induced interwell coherent tunneling in coupled quantum wells, the evolution of a one-dimensional envelope wave function $\phi(x,t)$ is determined by the time-dependent Schrödinger equation

$$H\phi(x,t)=i\hbar\frac{\partial}{\partial t}\phi(x,t), \tag{1}$$

with BenDaniel and Duke's effective Hamiltonian[11]

$$H=\frac{-\hbar^2}{2}\frac{\partial}{\partial x}\left[\frac{1}{m^*(x)}\frac{\partial}{\partial x}\right]+V(x), \tag{2}$$

so as to preserve the continuity of the wave function. The additional potential $|e|Fx$ due to the external electric field is added directly to the potential profile of the coupled-quantum-well structure. Equation (1) can be discretized with respect to time and space[10]

$$\frac{\phi_{j+1,n+1}}{m^*_{j+1}+m^*_j}+\left[\frac{2\epsilon^2}{\hbar\delta}i-\frac{\epsilon^2}{\hbar^2}V_j-\frac{1}{m^*_{j+1}+m^*_j}-\frac{1}{m^*_{j-1}+m^*_j}\right]\phi_{j,n+1}+\frac{\phi_{j-1,n+1}}{m^*_{j-1}+m^*_j}+\frac{\phi_{j+1,n}}{m^*_{j+1}+m^*_j}$$
$$-\left[\frac{2\epsilon^2}{\hbar\delta}i+\frac{\epsilon^2}{\hbar^2}V_j+\frac{1}{m^*_{j+1}+m^*_j}+\frac{1}{m^*_{j-1}+m^*_j}\right]\phi_{j,n}+\frac{\phi_{j-1,n}}{m^*_{j-1}+m^*_j}=0, \tag{3}$$

where ϵ, j, δ, and n are the space interval, space index, time interval, and time index, respectively. In the numerical calculations, the space interval ϵ and time interval δ are chosen to be 1 Å and 1 fsec (10^{-15}). With an initial wave function, Eq. (3) can be reduced to a standard $Ax=b$ matrix equation with A being a complex tridiagonal matrix. This matrix equation is solved by the Gaussian elimination method and time evolution can be obtained by iterative multiplication of the inverted matrix.

To determine the Stark shift in each well due to the electric field, the time-independent Schrödinger equation is employed, and is given by

$$H\phi(x)=E\phi(x). \tag{4}$$

With BenDaniel and Duke's effective Hamiltonian,[11] the time-independent Schrödinger equation is converted to[10]

$$\frac{-\hbar^2}{\epsilon^2}\left[\frac{\phi_{j+1}}{m^*_{j+1}+m^*_j}+\frac{\phi_{j-1}}{m^*_{j-1}+m^*_j}-\frac{\phi_j}{m^*_{j+1}+m^*_j}-\frac{\phi_j}{m^*_{j-1}+m^*_j}\right]+V_j\phi_j=E\phi_j, \tag{5}$$

using a standard central-differencing technique to ensure Hermiticity. The difference equation can be written in a matrix equation $\tilde{H}\Phi=E\Phi$. Multiplying a starting vector $\Phi^{(0)}$ by $(\tilde{H}-\mu I)^{-K}$, one obtains

$$(\tilde{H}-\mu I)^{-K}\Phi^{(0)}=\frac{a_1\Phi_1}{(E_1-\mu)^K}+\frac{a_2\Phi_2}{(E_2-\mu)^K}+\cdots+\frac{a_n\Phi_n}{(E_n-\mu)^K}, \tag{6}$$

where μ is an adjustable parameter, $\Phi_1, \Phi_2, \ldots, \Phi_n$ are the eigenvectors, and $E_1, E_2, \ldots, E_n$ are the eigenvalues of the matrix $\tilde{H}$. If μ is much closer to E_1 than to any other eigenvalue, $(\tilde{H}-\mu I)^{-K}\Phi^{(0)}$ will have a dominant component in the direction of Φ_1. Thus Eq. (6) can be approximated by

$$(\tilde{H}-\mu I)^{-K}\Phi^{(0)}\approx\frac{a_1\Phi_1}{(E_1-\mu)^K}. \tag{7}$$

As the number of iterations (K) becomes large, the eigenvector Φ_1 can be retrieved from the normalization condition and the eigenvalue E_1 can be retrieved from Φ_1. By varying μ over energies from the bottom to the top of each quantum well, the eigenvectors and eigenvalues can be found in succession.

III. APPLICATION TO COUPLED-QUANTUM-WELL SYSTEMS

First, coupled-quantum-well systems of 70-40-50 (first well width–barrier width–second well width in angstroms) with barrier height of 0.4 eV are studied. The effective masses are $0.067m_0$ in the well region and $0.1002m_0$ in the barrier region. The energy difference ΔE

is given by

$$\Delta E = E_{1F} - E_{2F} + F\left[p + \frac{l+q}{2}\right], \tag{8}$$

where l, p, and q denote the first well width, barrier width, and second well width in coupled quantum wells, respectively, E_{1F} and E_{2F} are the ground-state energies in the first and second wells, respectively, assuming that the two wells are isolated from each other, and F is the external electric field. A Stark shift in each well due to the external electric field is taken into consideration using the inverse power method described in Sec. II. Three external electric fields of 10, 33, and 60 kV/cm corresponding to ΔE's of -23.47, -0.478, and 26.26 meV (under bias, resonance, and over bias) in 70-40-50 coupled wells are chosen. The changes of $|E_1 - E_2|$'s due to the electric fields at 10, 33, and 60 kV/cm are small because both E_{1F} and E_{2F} shift to the same direction.

Figures 2–4 show the interwell tunneling in 70-40-50 coupled wells at under bias (10 kV/cm), resonance (33 kV/cm), and over bias (60 kV/cm) conditions, respectively. The initial wave function is the eigenfunction of the first well without the electric field, and the tunneling process is initiated by the onset of an applied electric field. This provides a detailed picture of the time-dependence of field-induced coherent tunneling in coupled quantum wells. In Fig. 2, the wave packet tunnels from the first well to the second well during the first 110 fsec. The first-well-peak to second-well-peak ratio is 10.3 at 110 fsec. However, as time increases, the wave packet tunnels back to the first well. The arrows in the figures indicate the oscillation of the wave packet. At resonance, as shown in Fig. 3, it takes much longer for the wave packet to reach the peak in the second well and then to tunnel back. In addition, the peak at the second well is much more significant (the peak to peak ratio is 0.72 at 800 fsec). As the electric field increases, shown in Fig. 4 at over bias, the tunneling cycle becomes much shorter and the peak to peak ratio becomes larger (14.1 at 14 fsec). This demonstrates resonant tunneling and nonresonant tunneling effects in coupled quantum wells.

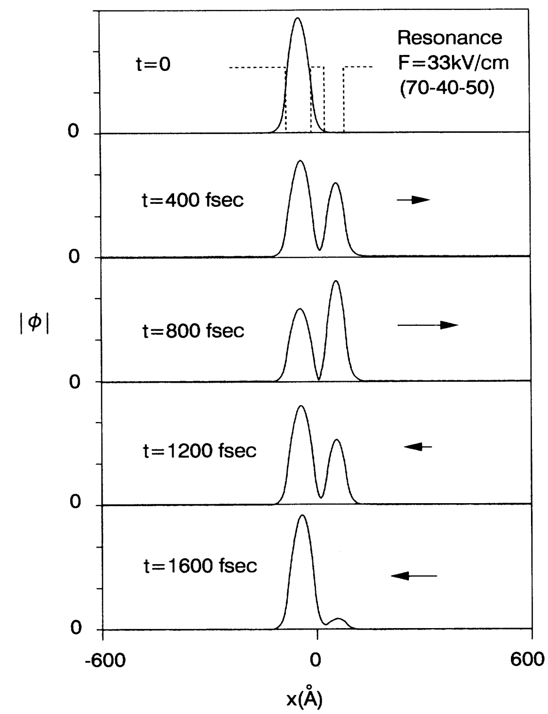

FIG. 3. An interwell coherent tunneling in 70-40-50 coupled quantum wells subject to an external electric field of 33 kV/cm (resonance). The position of the coupled quantum wells is shown by the dashed line at the $t=0$ frame. The arrows indicate the oscillation of the wave packet. At 400 and 800 fsec the wave packet tunnels into the second well while at 1200 and 1600 the wave packet tunnels back to the first well.

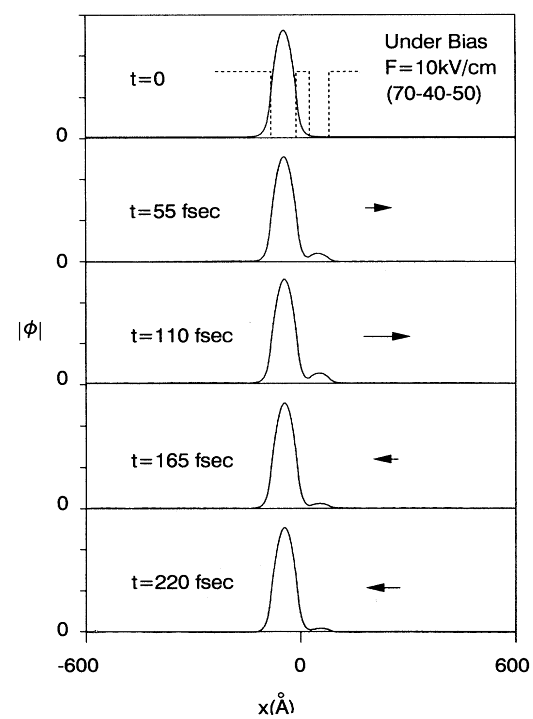

FIG. 2. An interwell coherent tunneling in 70-40-50 coupled quantum wells subject to an external electric field of 10 kV/cm (under bias). The position of the coupled quantum wells is shown by the dashed line at the $t=0$ frame. The arrows indicate the oscillation of the wave packet. At 55 and 110 fsec the wave packet tunnels into the second well while at 165 and 220 the wave packet tunnels back to the first well.

In order to characterize further the properties of interwell tunneling based on time-dependent analysis and to show the effects of the barrier width, the tunneling probability $P(t)$ (which represents the tunneling of a particle after a time t since the initialization of the tunneling process) can be defined using the overlap integral between two wave functions as[10]

$$P(t) = 1 - |\langle \phi(x,0) | \phi(x,t) \rangle|^2. \tag{9}$$

Figure 5 shows the tunneling probability at resonance for

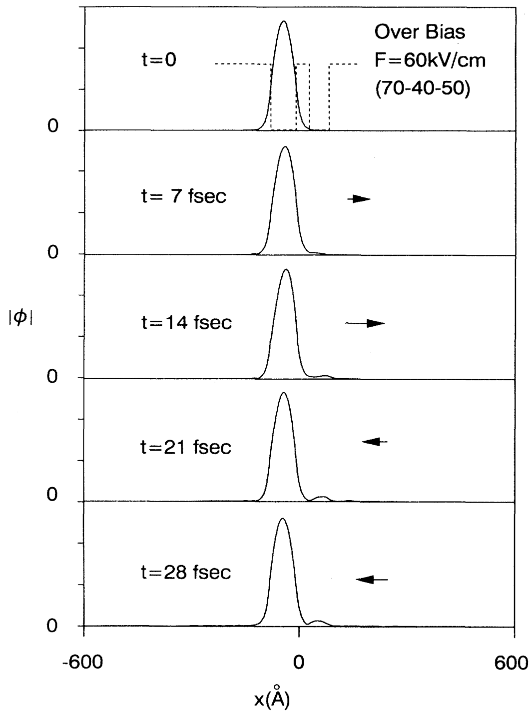

FIG. 4. An interwell coherent tunneling in 70-40-50 coupled quantum wells subject to an external electric field of 60 kV/cm (over bias). The position of the coupled quantum wells is shown by the dashed line at the $t=0$ frame. The arrows indicate the oscillation of the wave packet. At 7 and 14 fsec the wave packet tunnels into the second well while at 21 and 28 the wave packet tunnels back to the first well.

70-30-50 ($F=36.7$ kV/cm), 70-40-50 ($F=33$ kV/cm), and 70-50-50 ($F=30$ kV/cm) coupled-quantum-well systems. The electric fields for these three cases are chosen so that ΔE's are close (-0.475, -0.478, and -0.458 meV, respectively). In all cases, the particle tunnels into the second well very rapidly at the beginning. The tunneling process seems to slow down and then the particle slowly tunnels back to the first well. Again, the particle tunnels into the second well very rapidly as the beginning of the tunneling process. There is a very significant difference between tunneling into the second well and tunneling back to the first well. This shows that field-induced interwell coherent tunneling possesses an asymmetric oscillation effect.

In addition, Fig. 5 shows some properties and their dependence on the barrier width for close $|\Delta E|$'s. For a narrow barrier width (70-30-50), the tunneling cycle is shorter and the maximum tunneling probability is larger. This indicates that for a narrow barrier it takes a shorter time to tunnel through and a larger portion of the wave packet is involved in the tunneling process. Another interesting property associated with the coherent-tunneling effect in coupled quantum wells is the peak-to-valley ratio of the tunneling probability, which characterizes the amplitude of the oscillation. The typical peak-to-valley ratios for 70-30-50, 70-40-50, and 70-50-50 at resonance are 6.27, 3.58, and 2.45×10^2. A narrow barrier also gives a larger peak-to-valley ratio.

Figure 6 shows the tunneling probability at under bias conditions and for various barrier widths. The electric fields are 11.1, 10, and 9.1 kV/cm corresponding to ΔE's of -23.39, -23.37, and -23.36 meV for 70-30-50, 70-40-50, and 70-50-50 coupled quantum wells, respectively. The maximum tunneling probability in either case is much smaller in comparison with that at resonance. This indicates that, at under bias conditions, only a very small portion of the wave packet ever tunnels into the second well. For a wide barrier width (70-50-50), the peak-to-valley ratio is smaller. Actually, it is so small that the noise level becomes significant in this case.

At over bias conditions, the tunneling probability for various widths is shown in Fig. 7. The electric fields are 66.8, 60, and 54.5 kV/cm corresponding to ΔE's of 26.29, 26.26, and 26.27 meV for 70-30-50, 70-40-50, and 70-50-50 coupled quantum wells, respectively. Similarly, the maximum tunneling probability in all cases is much

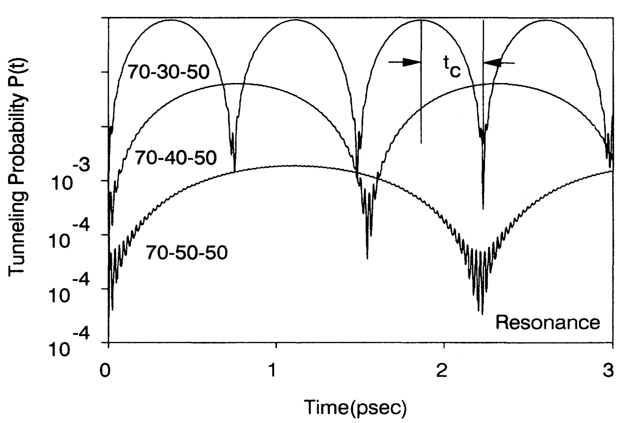

FIG. 5. Tunneling probability defined by Eq. (9) for coupled quantum wells with various barrier widths at resonance. The applied electric fields are 36.7, 33, and 30 kV/cm corresponding to ΔE's of -0.475, -0.478, and -0.46 meV for 70-30-50, 70-40-50, and 70-50-50 coupled quantum wells, respectively.

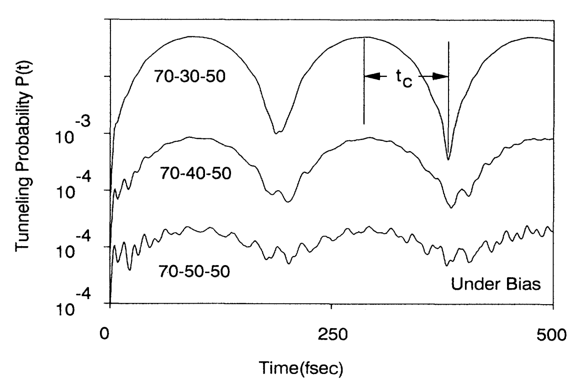

FIG. 6. Tunneling probability defined by Eq. (9) for 70-40-50 coupled quantum wells at under bias conditions. The applied electric fields are 11.1, 10, and 9.1 kV/cm corresponding to ΔE's of -23.39, -23.37, and -23.36 meV for 70-30-50, 70-40-50, and 70-50-50 coupled quantum wells, respectively.

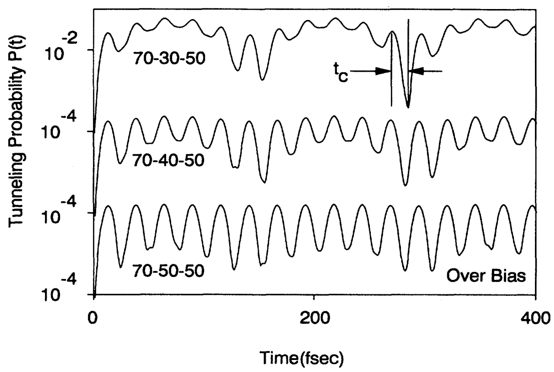

FIG. 7. Tunneling probability defined by Eq. (9) for 70-40-50 coupled quantum wells at over bias conditions. The applied electric fields are 66.8, 60, and 54.5 kV/cm corresponding to ΔE's of 26.29, 26.26, and 26.27 meV for 70-30-50, 70-40-50, and 70-50-50 coupled quantum wells, respectively.

smaller in comparison with that at resonance. In addition, the local minimum of the tunneling probability changes in each tunneling cycle. It seems to repeat itself every six to seven tunneling cycles. This effect is more significant in a narrow barrier width (70-30-50).

IV. COMPARISON TO THE CONVENTIONAL MODEL

In the conventional model, the evolution of the wave function in coupled quantum wells is given by[9]

$$\phi(t)=e^{-iE_0t/\hbar}[(\phi_{\rm II}+\phi_{\rm IV})e^{i\delta Et/\hbar}+(\phi_{\rm II}-\phi_{\rm IV})e^{-i\delta Et/\hbar}], \tag{10}$$

where $\phi_{\rm II}$ and $\phi_{\rm IV}$ refer to the wave function in the first and second wells, respectively, and $\phi_{\rm II}\pm\phi_{\rm IV}$ has energy $E_0\mp\delta E$. The δE is obtained from the eigenvalue equation of a symmetric coupled-quantum-well system using the first-order perturbation technique. The coherent-tunneling time t_c is defined as a time interval giving a $\pi/2$ phase change, and is[6,7,9]

$$t_c=\frac{\hbar\pi}{2|\delta E|}=\frac{h}{2|\Delta E|}. \tag{11}$$

This coherent-tunneling time represents the time for the wave function to change phase such that $\phi(0)\sim\phi_{\rm II}$ and $\phi(t_c)\sim\phi_{\rm IV}$, where the two states are separated by $|\Delta E|$ or $2|\delta E|$.

There are several disadvantages using Eq. (11). The first one is that Eq. (11) is valid only when ΔE is small, namely, at resonance. At nonresonance, ΔE is large and the perturbation technique is inappropriate to determine ΔE. However, in the time-dependent analysis, ΔE is calculated using the inverse power method. This approach without the assumption of small ΔE is more appropriate for at resonance and nonresonance in coupled quantum wells. Also, electric-field effects are not taken into consideration in the conventional model since the evolution of the wave function using Eq. (10) depends only on ΔE. In contrast to the conventional model, the evolution of the wave function in the time-dependent analysis is described by the application of the time-dependent Schrödinger equation, where the external electric field is included in the effective Hamiltonian [see Eq. (2)]. In addition, the conventional model uses the phase change in time in both wells to describe the spatial-tunneling effects. This approach has the conceptual disadvantage of not using the probability distribution function $|\phi(x,t)|^2$, which is the probability that the particle at time t be found in the region between x and $x+dx$. Thus it is more logical to use the probability distribution function $|\phi|^2$ to describe the spatial coherent tunneling than the phase change of the wave function.

At resonance, it is desirable to compare the coherent-tunneling time based on the time-dependent analysis to the conventional model. As shown in Fig. 5, a seasonable way is to define the time required for a particle to reach from a local maximum to the next local minimum as the coherent-tunneling time. Table I lists the coherent-tunneling time at resonance for 70-30-50, 70-40-50, and 70-50-50 coupled-quantum-well systems obtained from the conventional model and from the time-dependent analysis. It is shown that in the time-dependent analysis the tunneling time changes significantly as the barrier width varies. This effect is lost if the coherent tunneling is simply characterized by Eq. (11). Also, the conventional model gives a poor prediction of the tunneling time at resonance. It is because the external electric field is not taken into consideration in the conventional analysis. By including the electric-field effects in the time-dependent analysis, the coherent tunneling becomes a much faster process.

At nonresonance, the coherent-tunneling time based on the time-dependent analysis can be obtained in a similar way and then compared to the conventional model, as shown in Table I. However, it should be pointed out that

TABLE I. Comparison of the coherent-tunneling time t_c in femtoseconds (10^{-15}) of an electron wave packet in 70-30-50, 70-40-50, and 70-50-50 coupled quantum wells at under bias, resonance, and over bias conditions obtained from the conventional model [Eq. (11)] and the time-dependent analysis (Figs. 5–7).

t_c	Conventional model	Time-dependent analysis		
(10^{-15} sec)	all cases	70-30-50	70-40-50	70-50-50
Under bias	88	97	105	104
Resonance	4380	375	760	1110
Over bias	97	9	11	12

some properties could be overlooked in such a simple comparison. For example, the peak-to-valley ratio is small and only a very small portion of the wave packet ever tunnels into the second well. At over bias conditions, the local minimum of the tunneling probability changes in each tunneling cycle. In comparison to the conventional model, the time-dependent analysis provides a more detailed picture and shows a significant difference in coherent time between under bias and over bias conditions. It is because the particle carries a significant amount of momentum at over bias conditions. Thus the coherent time is shorter. Again, this effect is overlooked by the conventional model.

V. CONCLUSIONS

Compared to the conventional model currently in use, the method presented in this work offers a more accurate solution to the Schrödinger equation in representing interwell coherent tunneling in coupled quantum wells. Time evolution of the wave packet in the coupled quantum wells is shown by a numerical implementation of the time-development operator of the Schrödinger equation. Some improvements include (1) being able to describe the process at resonance and nonresonance, (2) consideration of the external electric field, and (3) using the probability density function $|\phi|^2$ to describe the spatial-tunneling effect. In addition, this approach provides a detailed time-dependent picture of field-induced coherent tunneling in coupled quantum wells and shows several effects that are overlooked by the conventional model.

ACKNOWLEDGMENT

This work was supported in part by the Ministry of Economic Affairs of R.O.C. under Project No. 34P1200.

[1] R. Dingle, A. C. Gossard, and W. Wiegmann, Phys. Rev. Lett. **34**, 1327 (1975).

[2] H. Kawai, I. Hase, K. Kaneko, and N. Watanabe, J. Cryst. Growth **68**, 406 (1984).

[3] H. Q. Le, J. J Zayhowski, and W. D. Goodhue, Appl. Phys. Lett. **50**, 1518 (1987).

[4] Y. J. Chen, E. S. Koteles, B. S. Elman, and C. A. Armiento, Phys. Rev. B **36**, 4562 (1987).

[5] S. Tarucha, K. Ploog, and K. v. Klitzing, Phys. Rev. B **36**, 4558 (1990).

[6] D. Y. Oberli, J. Shah, T. C. Damen, C. T. Wu, T. Y. Chang, D. A. B. Miller, J. E. Henry, R. F. Kopf, N. Sauer, and A. E. DiGiovanni, Phys. Rev. B **40**, 3028 (1989).

[7] N. Shimizu, T. Furuta, T. Waho, and T. Mizutani, Jpn. J. Appl. Phys. **29**, L1757 (1990).

[8] D. Y. Oberli, J. Shah, T. C. Damen, J. M. Kuo, J. E. Henry, J. Lary, and S. M. Goodnick, Appl. Phys. Lett. **56**, 1239 (1990).

[9] E. O. Kane, in *Tunneling Phenomena in Solids,* edited by E. Burstein and S. Lundqvist (Plenum, New York, 1969), Chap. 1.

[10] C. Juang, K. J. Kuhn, and R. B. Darling, Phys. Rev. B **41** 12 047 (1990).

[11] D. J. BenDaniel and C. B. Duke, Phys. Rev. **152**, 683 (1966).